Supporting Information

Polyvinylpyrrolidone Gel Based Pt/Ni(OH)$_2$ Heterostructures with Redistributing Charges for Enhanced Alkaline Hydrogen Evolution Reaction

Jin Li[†],[a] Bo Li[†],[b] He Huang[*],[b,c] Shuo Yan,[a] Changzhou Yuan[*],[d] Naiteng Wu,[a] Donglei Guo,[a] Xianming Liu[*a]

[a]*College of Chemistry and Chemical Engineering, and Henan Key Laboratory of Function-Oriented Porous Materials, Luoyang Normal University, Luoyang 471934, E-mail: myclxm@163.com*

[b]*School of Materials Science and Engineering, University of Science and Technology Beijing, Beijing 100083, China*

[c]*Department of Mechanical and Aerospace Engineering, Hong Kong University of Science and Technology, Clear Water Bay, Kowloon, Hong Kong, China, E-mail:hhuangae@connect.ust.hk*

[d]*School of Materials Science & Engineering, University of Jinan, Jinan, 250022 P. R. China, E-mail: mse_yuancz@ujn.edu.cn*

[†]*These authors contributed equally to this work*

**Corresponding authors*

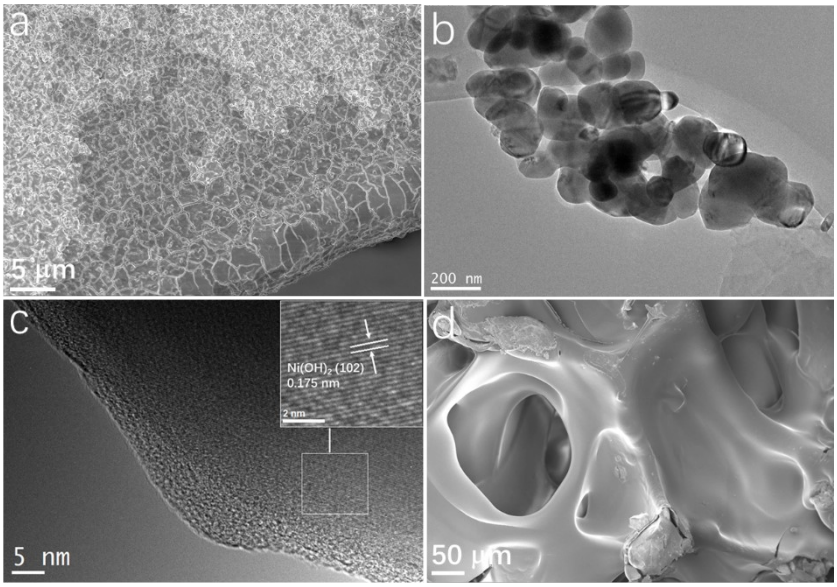

Figure S1. (a) FESEM, (b) TEM and (c) HRTEM images of $Ni(OH)_2$. (d) FESEM image of PVP@NF.

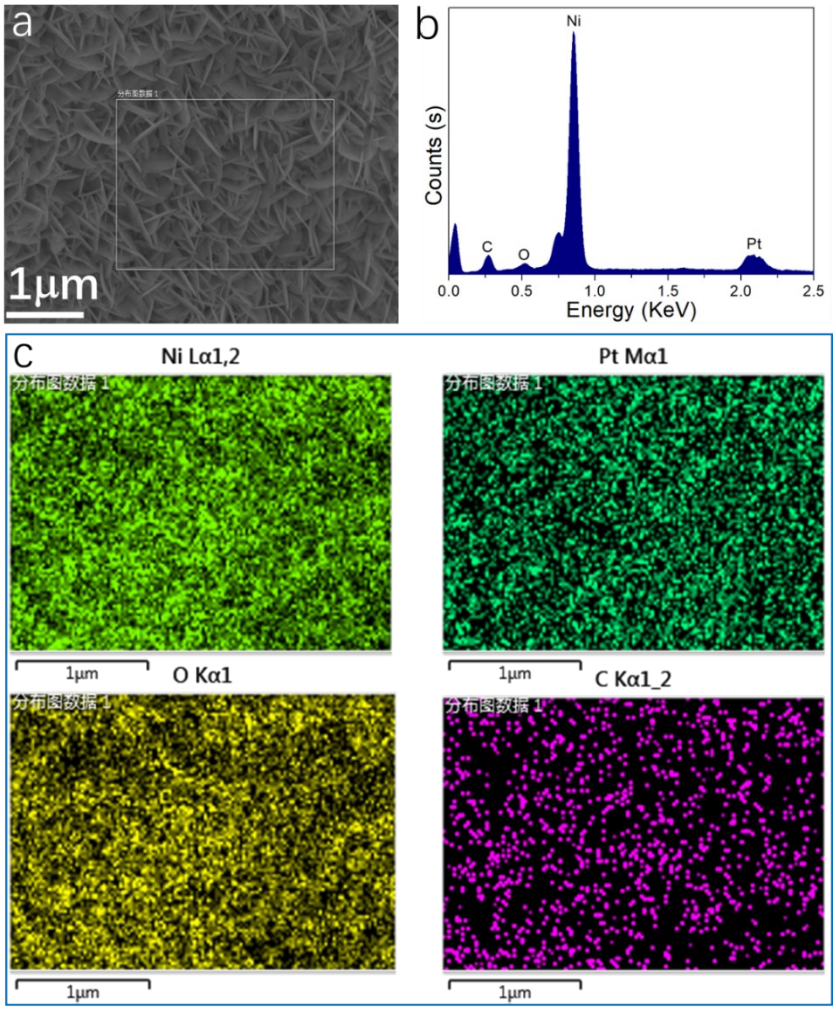

Figure S2. (a) FESEM, (b) EDX and (c) the corresponding elemental mapping images of Pt/Ni(OH)$_2$@NF.

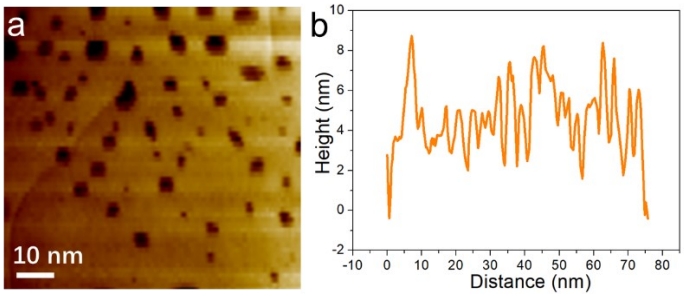

Figure S3. (a) High-resolution AFM image and (b) thickness profile of PVP@Pt/Ni(OH)$_2$@NF sample.

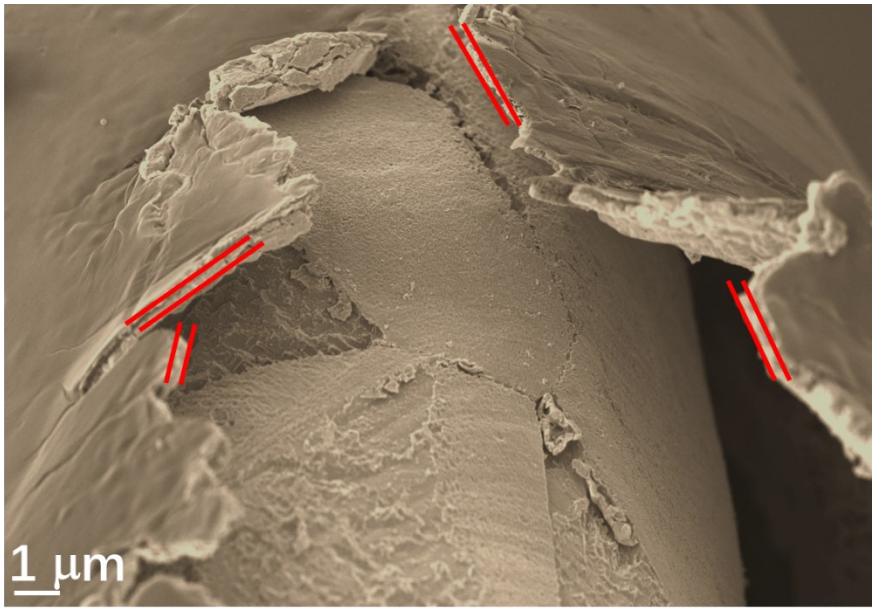

Figure S4. The FESEM images of PVP@Pt/Ni(OH)$_2$@NF sample.

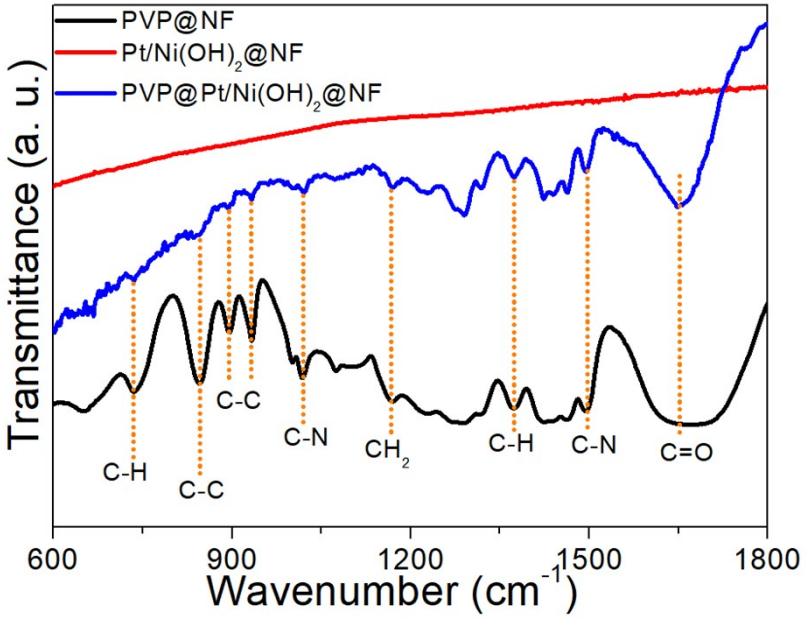

Figure S5. FTIR spectra of PVP@NF, Pt/Ni(OH)$_2$@NF and PVP@Pt/Ni(OH)$_2$@NF.

Typical peaks of PVP can be observed in the PVP@NF and PVP@Pt/$Ni(OH)_2$@NF spectrum, in detail: symmetric C=O stretching modes at 1650 cm^{-1}, C-N ring stretching mode at 1496 cm^{-1}, C-H bending mode at 1373 cm^{-1}, weak ring CH_2 twisting mode at 1168 cm^{-1}, C-N stretching mode at 1020 cm^{-1}, C-C ring breathing mode at 932 cm^{-1}, C-C ring mode at 894 cm^{-1}, out-of-plane C-H bending mode at 846 cm^{-1}, and C-H rocking mode at 734 cm^{-1}.[1, 2]

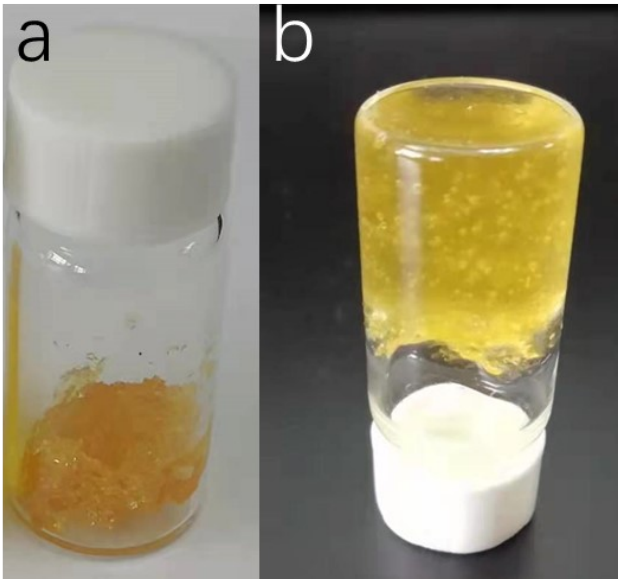

Figure S6. The photograph of (a) PVP gels scraped from PVP@Pt/$Ni(OH)_2$@NF and (b) the corresponding hydrogels after swelling.

Figure S7. The typical optical photographs before and after HER test for PVP@Pt/Ni(OH)$_2$@NF

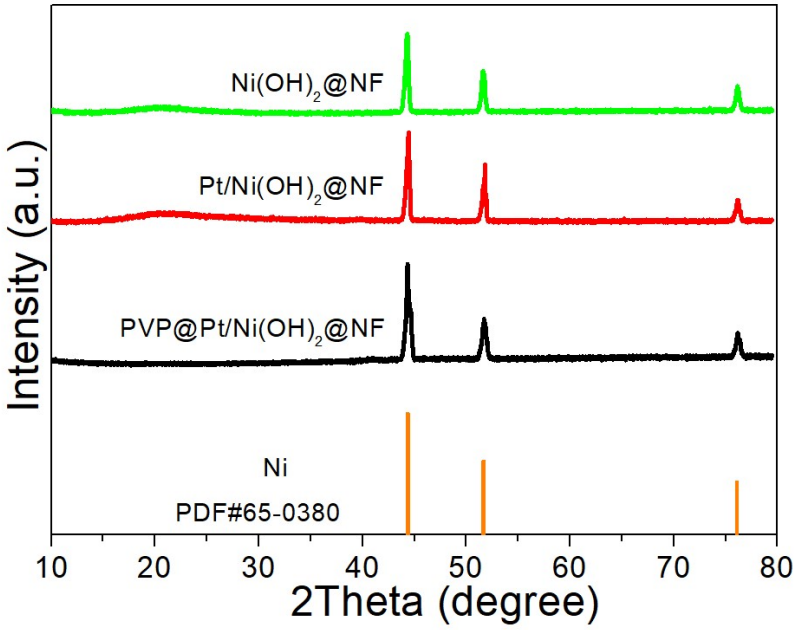

Figure S8. XRD pattern of Ni(OH)$_2$@NF, Pt/Ni(OH)$_2$@NF, PVP@Pt/Ni(OH)$_2$@NF and the standard PDF card of Ni (orange line).

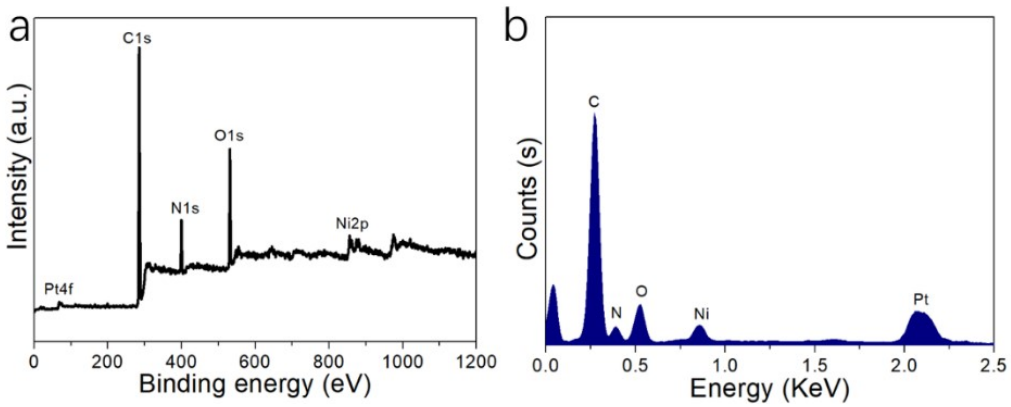

Figure S9. XPS survey and EDX spectrum of PVP@Pt/Ni$(OH)_2$@NF.

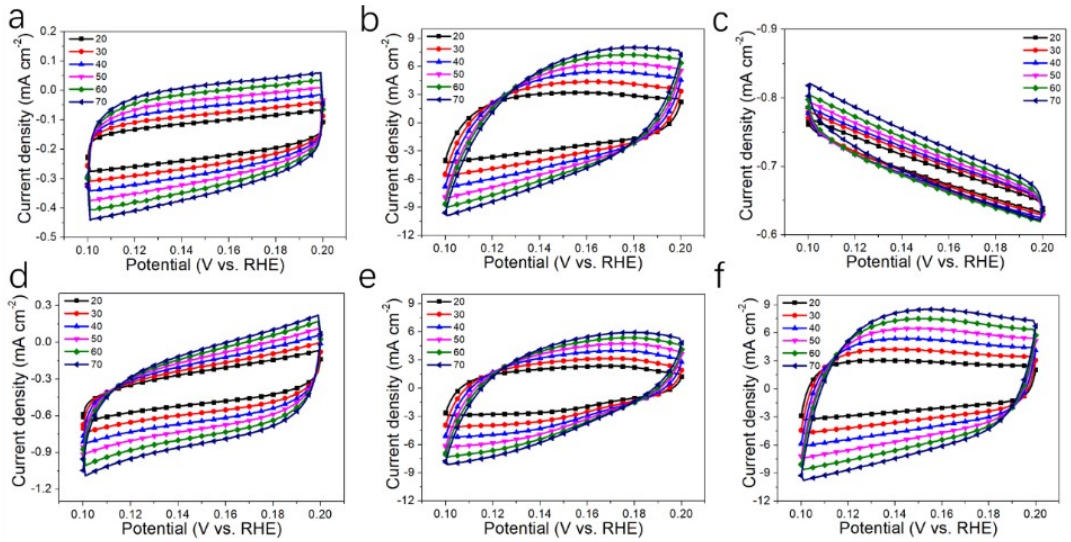

Figure S10. CV curves of (a) NF, (b) Pt/C, (c) PVP@NF, (d) $Ni(OH)_2$@NF, (e) Pt/$Ni(OH)_2$@NF, and (f) PVP@Pt/$Ni(OH)_2$@NF measured in a non-Faradic region at the scan rates of 20, 30, 40, 50, 60, and 70 mV s^{-1}.

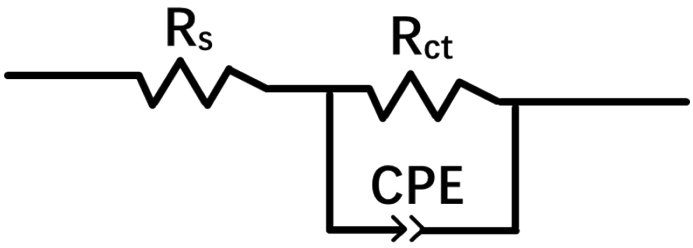

Figure S11. The equivalent circuit models.

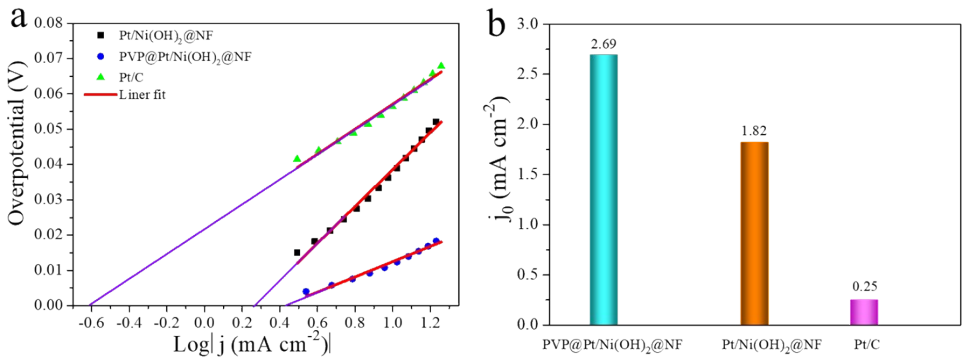

Figure S12. Exchange current densities (j_0) of the PVP@Pt/Ni(OH)$_2$@NF, Pt/Ni(OH)$_2$@NF, and commercial Pt/C catalysts in 1.0 M KOH.

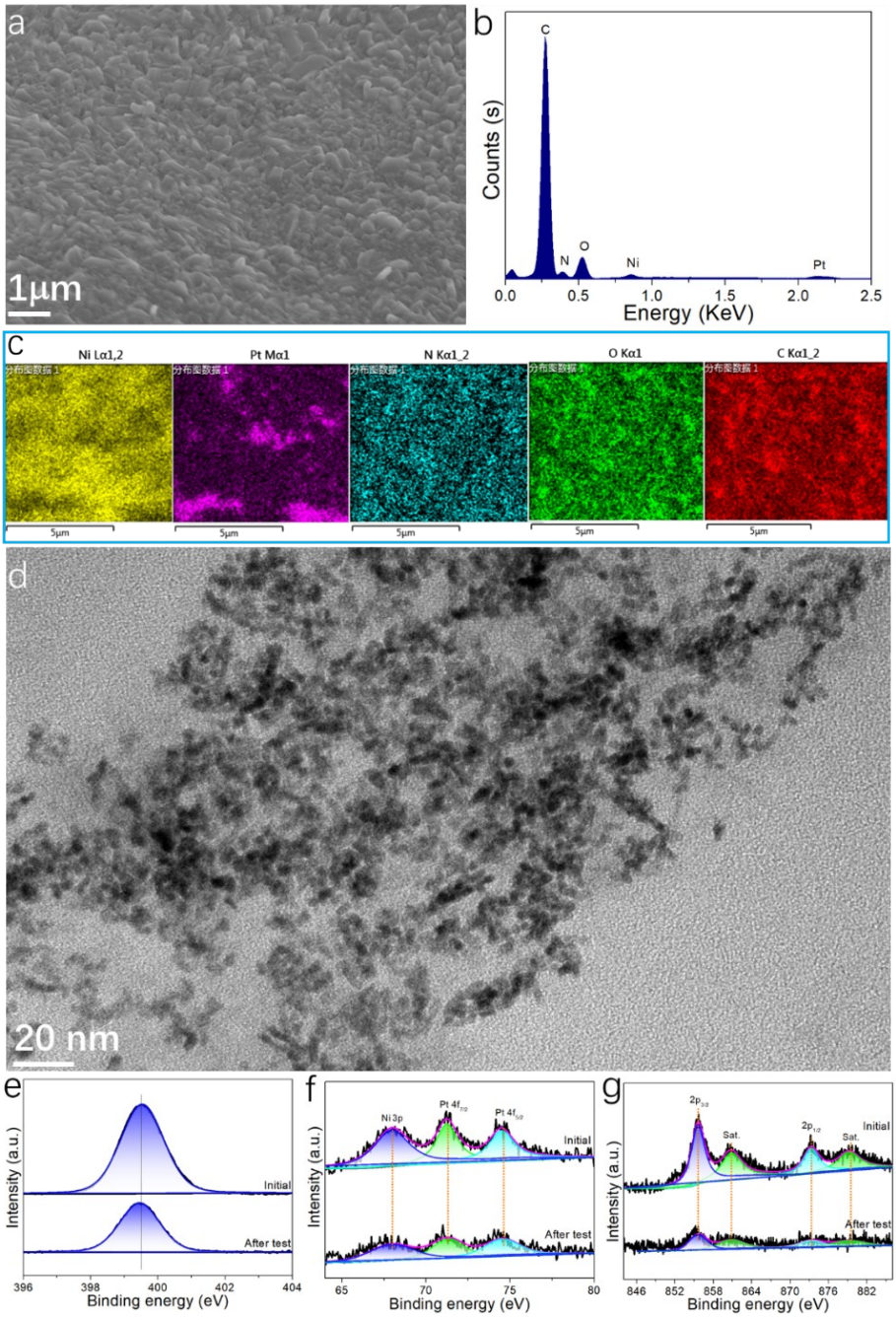

Figure S13. (a) FESEM, (b)EDX, (c) the corresponding elemental mapping images and (d) TEM of PVP@Pt/$Ni(OH)_2$@NF after stability test. XPS spectra of (e) N1s, (f) Pt 4f and (g) Ni 2p for PVP@Pt/$Ni(OH)_2$@NF before and after the durability tests.

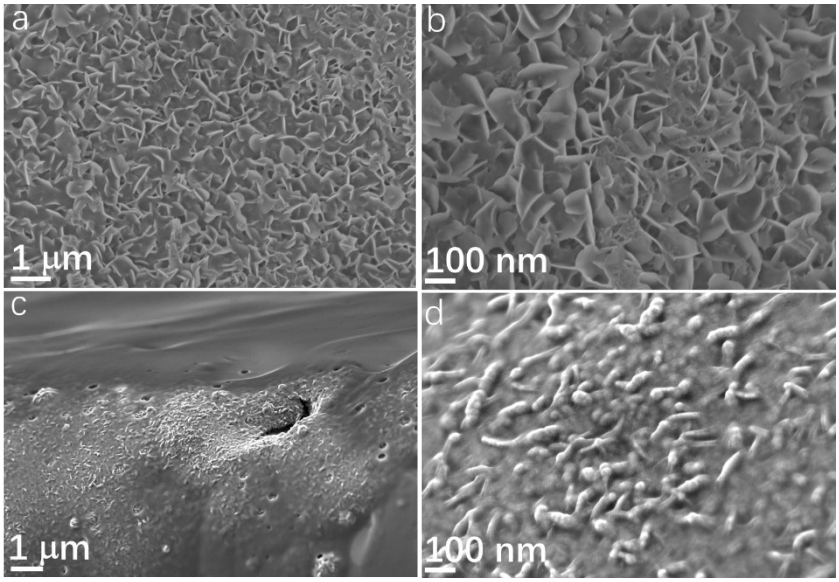

Figure S14. The FESEM images of PVP@Pt/Ni(OH)$_2$@NF with 40 mg PVP (a,b) and 70 mg PVP (c,d).

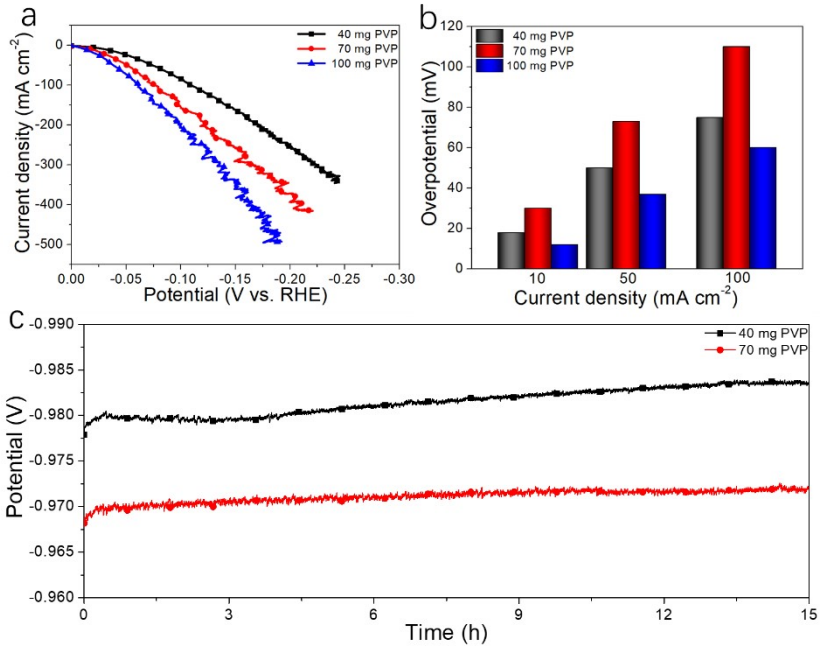

Figure S15. (a) LSV curves and (b) overpotentials of PVP@Pt/Ni(OH)$_2$@NF prepared with 40, 70, and 100 mg PVP. (c) Chronopotentiometry test of PVP@Pt/Ni(OH)$_2$@NF prepared with 40 and 70 mg PVP at 10 mA cm^{-2} for 15 h without *IR* compensation.

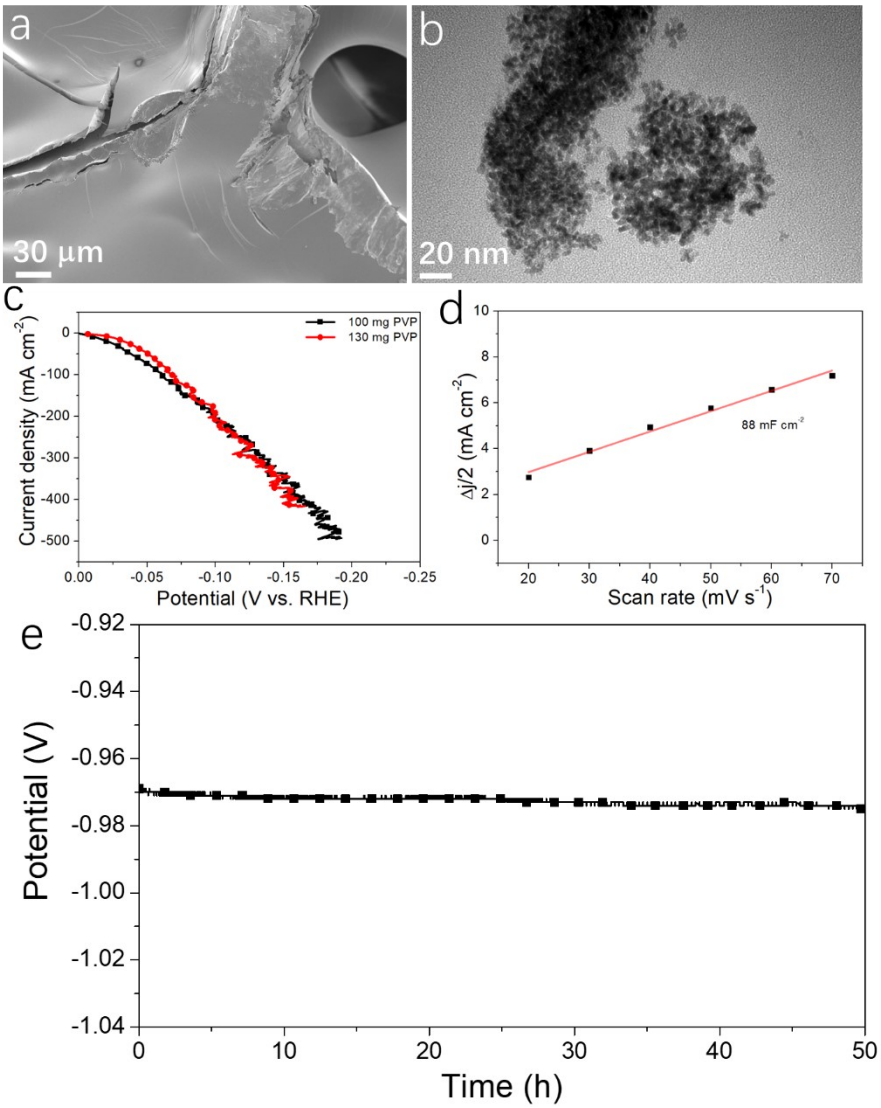

Figure S16. The FESEM (a) and TEM (b) images of PVP@Pt/$Ni(OH)_2$@NF prepared with 130 mg PVP. (c) The corresponding LSV curves, (d) electrochemical double-layer capacitances, and (e) Chronopotentiometry test at 10 mA cm^{-2} for 50 h without *IR* compensation.

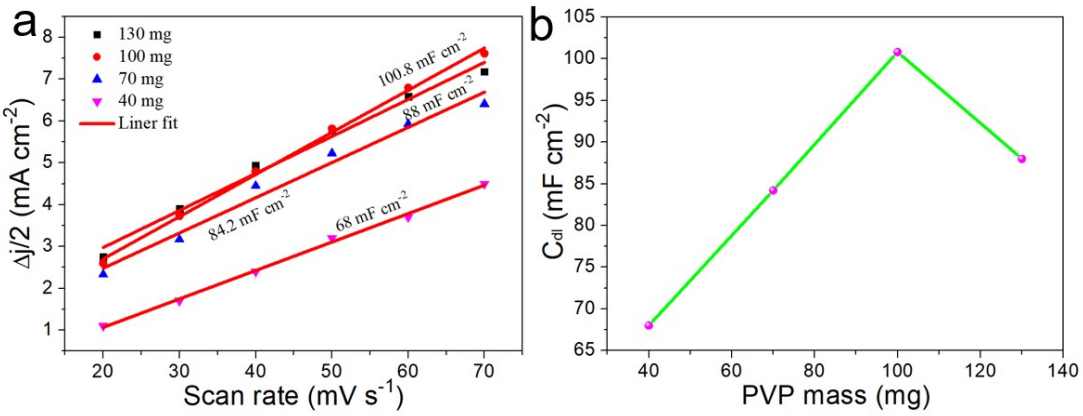

Figure S17. (a) The electrochemical double-layer capacitances for different PVP mass. (b) The plot of the relationships between PVP mass and electrochemical double-layer capacitances.

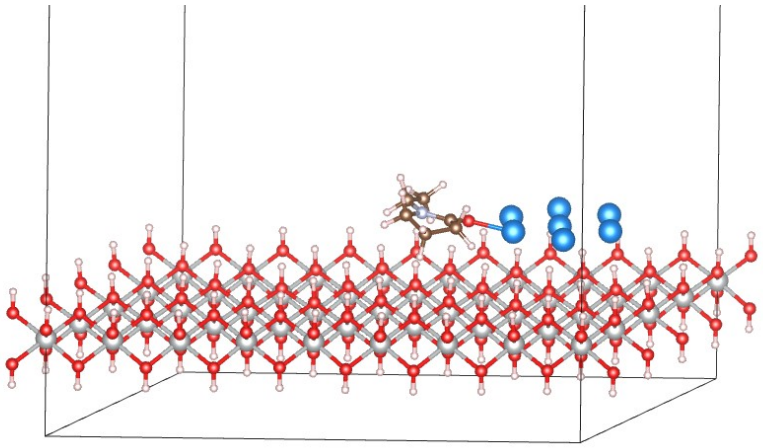

Figure S18. Optimized configuration of PVP@Pt/Ni(OH)$_2$ catalyst surface. The silver, red, pink, blue, brown, and orange balls represent Ni, O, H, Pt, C, and N atoms, respectively.

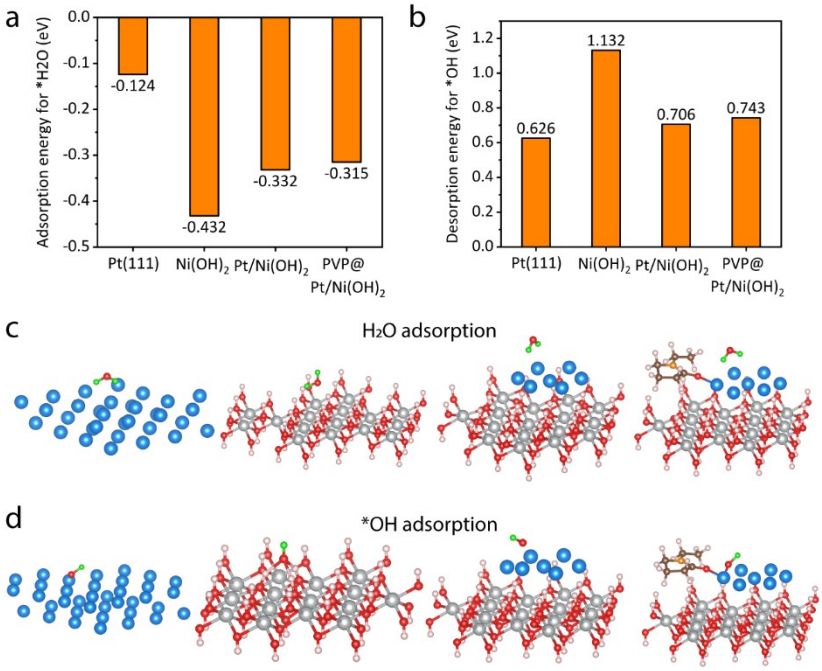

Figure S19. (a) Adsorption energies of H_2O and (b) desorption energies of OH. (c) and (d) exhibit the corresponding optimized configurations.

Table S1. The HER performance of PVP@Pt/Ni(OH)$_2$@NF compared with other catalysts at a current density of 10 mA cm^{-2} in 1.0 M KOH.

Catalysts	Overpotential (mV)	Tafel slope (mV dec^{-1})	References
PVP@Pt/Ni(OH)$_2$@NF	12	21.5	This work
PtNi$_5$-0.3	12.8	14.1	[3]
RuNi/CQDs	13	48	[4]
Ni$_3$N/Pt	50	36.5	[5]
MoP@NCHs	92	62	[6]
Pt-Co(OH)$_2$/CC	32	70	[7]
Co-NMS/CA	89	62	[8]
PtNi-O/C	39.8	78.8	[9]
Ru/Ni(OH)$_2$/NF	25	47	[10]
Pt-Ni ASs	27.7	27	[11]
Pt-Ni(N) NWs	13	29	[12]
Ru-MoO$_2$	44	29	[13]
Pt$_2$Ni$_3$-P	44	66	[14]
Pt/NiRu-OH	38	29	[15]
RuNi NSs	15	28	[16]
Pt@Fe-N-C	60	42	[17]
Ru/OMSNNC	13	40.41	[18]
PtNi@Ti$_3$C$_2$	36	59	[19]
Ru@MWCNT	17	27	[20]
Ni$_{17}$W$_3$/WO$_2$	48	33	[21]
Ni$_2$P-NiSe$_2$	66	72.6	[22]
Co-Mo$_5$N$_6$	19	29	[23]
DSIrNi@CNTS	17	10	[24]
Pt$_{at}$-CoP MNSs/CFC	13	30.28	[25]
ES-WC/W$_2$C	75	59	[26]

$RhSe_2$	81.6	96	[27]
Ru-NBCs	14	36.19	[28]
CoP NS/CNTs	68	51	[29]
3D RuCu NCs	18	59	[30]
PtRu NCs/BP	22	19	[31]

Table S2. Fitting parameters acquired from the EIS data with Zview software for electrocatalysts in the alkaline HER.

Electrocatalyst	R_s (Ω)	R_{ct} (Ω)	CPE-T	CPE-P
NF	2.68	338.4	0.007	0.83
Pt/C	3.15	2.81	0.03	0.71
PVP@NF	4.05	120.6	0.01	0.47
$Ni(OH)_2$@NF	2.86	60.8	0.001	0.79
Pt/$Ni(OH)_2$@NF	2.12	3.38	0.01	0.76
PVP@Pt/$Ni(OH)_2$@NF	2.72	0.85	0.04	0.61

R_s = solution resistance; R_{ct} = charge transfer resistance; CPE-T/CPE-P = constant phase element.

References for the supporting information

1. M. Contardi, D. Kossyvaki, P. Picone, M. Summa, X. Guo, J. A. Heredia-Guerrero, D. Giacomazza, R. Carzino, L. Goldoni, G. Scoponi, F. Rancan, R. Bertorelli, M. Di Carlo, A. Athanassiou and I. S. Bayer, *Chem. Eng. J.*, 2021, **409**, 128144.
2. A. Kedia and P. S. Kumar, *The Journal of Physical Chemistry C*, 2012, **116**, 23721-23728.
3. C. Zhang, X. Liang, R. Xu, C. Dai, B. Wu, G. Yu, B. Chen, X. Wang and N. Liu, *Adv. Funct. Mater.*, 2021, **31**, 2008298.
4. Y. Liu, X. Li, Q. Zhang, W. Li, Y. Xie, H. Liu, L. Shang, Z. Liu, Z. Chen, L. Gu, Z. Tang, T. Zhang and S. Lu, *Angew. Chem. Int. Ed.*, 2020, **59**, 1718-1726.
5. Y. Wang, L. Chen, X. Yu, Y. Wang and G. Zheng, *Adv. Funct. Mater.*, 2017, **7**, 1601390.
6. D. Zhao, K. Sun, W. C. Cheong, L. Zheng, C. Zhang, S. Liu, X. Cao, K. Wu, Y. Pan, Z. Zhuang, B. Hu, D. Wang, Q. Peng, C. Chen and Y. Li, *Angew. Chem.*, 2019, **132**, 9067-9075.
7. Z. Xing, C. Han, D. Wang, Q. Li and X. Yang, *ACS Catal.*, 2017, **7**, 7131-7135.
8. L. Zhang, Y. Zheng, J. Wang, Y. Geng, B. Zhang, J. He, J. Xue, T. Frauenheim and M. Li, *Small*, 2021, **17**, e2006730.
9. Z. Zhao, H. Liu, W. Gao, W. Xue, Z. Liu, J. Huang, X. Pan and Y. Huang, *J. Am. Chem. Soc.*, 2018, **140**, 9046-9050.
10. Q.-Q. Chen, X. Yang, C.-C. Hou, K. Li and Y. Chen, *J. Mater. Chem. A*, 2019, **7**, 11062-11068.
11. Z. Zhang, G. Liu, X. Cui, B. Chen, Y. Zhu, Y. Gong, F. Saleem, S. Xi, Y. Du, A. Borgna, Z. Lai, Q. Zhang, B. Li, Y. Zong, Y. Han, L. Gu and H. Zhang,

Adv. Mater., 2018, **30**, e1801741.
12. Y. Xie, J. Cai, Y. Wu, Y. Zang, X. Zheng, J. Ye, P. Cui, S. Niu, Y. Liu, J. Zhu, X. Liu, G. Wang and Y. Qian, *Adv. Mater.*, 2019, **31**, e1807780.
13. F. Yu, H. Zhou, Y. Huang, J. Sun, F. Qin, J. Bao, W. A. Goddard, S. Chen and Z. Ren, *Nat. Commun.*, 2018, **9**, 2551.
14. P. Wang, Q. Shao, J. Guo, L. Bu and X. Huang, *Chem. Mater.*, 2020, **32**, 3144-3149.
15. D. Li, X. Chen, Y. Lv, G. Zhang, Y. Huang, W. Liu, Y. Li, R. Chen, C. Nuckolls and H. Ni, *Appl. Catal., B-Environ.*, 2020, **269**, 118824.
16. G. Liu, W. Zhou, B. Chen, Q. Zhang, X. Cui, B. Li, Z. Lai, Y. Chen, Z. Zhang, L. Gu and H. Zhang, *Nano Energy*, 2019, **66**, 104173.
17. X. Zeng, J. Shui, X. Liu, Q. Liu, Y. Li, J. Shang, L. Zheng and R. Yu, *Adv. Funct. Mater.*, 2018, **8**, 1701345.
18. Y. L. Wu, X. Li, Y. S. Wei, Z. Fu, W. Wei, X. T. Wu, Q. L. Zhu and Q. Xu, *Adv. Mater.*, 2021, **33**, 2006965.
19. Y. Yan, R. Zhang, Y. Yu, Z. Sun, R. Che, B. Wei, A. P. LaGrow, Z. Wang and W. Zhou, *Appl. Catal., B-Environ.*, 2021, **291**, 120100.
20. D. H. Kweon, M. S. Okyay, S. J. Kim, J. P. Jeon, H. J. Noh, N. Park, J. Mahmood and J. B. Baek, *Nat. Commun.*, 2020, **11**, 1278.
21. W. Xu, B. Wang, X. Ni, H. Liu, W. Wang, L. Zhang, H. Zhang, Z. Peng and Z. Liu, *ACS Appl. Mater. Interfaces*, 2021, **13**, 13838-13847.
22. C. Liu, T. Gong, J. Zhang, X. Zheng, J. Mao, H. Liu, Y. Li and Q. Hao, *Appl. Catal., B-Environ.*, 2020, **262**, 118245.
23. F. Lin, Z. Dong, Y. Yao, L. Yang, F. Fang and L. Jiao, *Adv. Funct. Mater.*, 2020, **10**, 2002176.
24. S. Liu, Z. Hu, Y. Wu, J. Zhang, Y. Zhang, B. Cui, C. Liu, S. Hu, N. Zhao, X. Han, A. Cao, Y. Chen, Y. Deng and W. Hu, *Adv. Mater.*, 2020, **32**, e2006034.
25. S. Ye, W. Xiong, P. Liao, L. Zheng, X. Ren, C. He, Q. Zhang and J. Liu, *J. Mater. Chem. A*, 2020, **8**, 11246-11254.
26. Z. Chen, W. Gong, S. Cong, Z. Wang, G. Song, T. Pan, X. Tang, J. Chen, W. Lu and Z. Zhao, *Nano Energy*, 2020, **68**, 104335.
27. W. Zhong, B. Xiao, Z. Lin, Z. Wang, L. Huang, S. Shen, Q. Zhang and L. Gu, *Adv. Mater.*, 2021, **33**, 2007894.
28. T. Wu, J. Hong, Z. Lu, H. Wu, C. Wu, Z. Tang, X. Liu, B. Zeng, Y. Xu, G. Chen, C. Yuan and L. Dai, *Appl. Catal., B-Environ.*, 2021, **285**, 119795.
29. Y. Zhang, Y. Wang, T. Wang, N. Wu, Y. Wang, Y. Sun, L. Fu, Y. Du and W. Zhong, *Adv. Mater. Interfaces*, 2019, **7**, 1901302.
30. D. Cao, J. Wang, H. Xu and D. Cheng, *Small*, 2020, **16**, 2000924.
31. Y. Li, W. Pei, J. He, K. Liu, W. Qi, X. Gao, S. Zhou, H. Xie, K. Yin, Y. Gao, J. He, J. Zhao, J. Hu, T.-S. Chan, Z. Li, G. Zhang and M. Liu, *ACS Catal.*, 2019, **9**, 10870-10875.